

# Time-Resolved CO<sub>2</sub> Dissociation in a Nanosecond Pulsed Discharge

Luca Matteo Martini<sup>1</sup>  · Sara Lovascio<sup>1</sup> · Giorgio Dilecce<sup>1,2</sup>  · Paolo Tosi<sup>1</sup> 

Received: 31 October 2017 / Accepted: 4 April 2018 / Published online: 10 May 2018  
© Springer Science+Business Media, LLC, part of Springer Nature 2018

**Abstract** Electrical discharges are increasingly used to dissociate CO<sub>2</sub> in CO and O<sub>2</sub>. This reaction is the first step in the way for the synthesis of value-added compounds from CO<sub>2</sub> by using renewable electricity. If efficient, this technology might allow at the same time recycling CO<sub>2</sub> and storing renewable energy in chemical form. At present, while the dissociation degree is measured in the reactor exhaust, little is experimentally known about the dissociation kinetics in the discharge and post-discharge. This knowledge is however critical to increasing the overall efficiency of the plasma process. To estimate the time dependence of the CO<sub>2</sub> dissociation following a discharge event, we have coupled a LIF diagnostics to a nanosecond repetitively pulsed discharge in a mixture of CO<sub>2</sub> and H<sub>2</sub>O. This paper discusses a procedure to obtain data on the time evolution of the CO<sub>2</sub> dissociation, its limits and future perspectives. In addition, the local gas temperature is measured as well. We find that a few microseconds after the discharge pulse, CO<sub>2</sub> is highly dissociated with a temperature around 2500 K. In about 100 μs, the temperature decreases at about 1500 K while the dissociation is reduced by about a factor of three.

**Keywords** Nanosecond repetitively pulsed discharge · CO<sub>2</sub> conversion · Energy storage · Laser-induced fluorescence

## Introduction

If driven by renewable energy, the efficient conversion of CO<sub>2</sub> into fuels and value-added products would be a tremendous step forward towards a sustainable energy scenario and an economy less dependent on fossil fuels [1]. In fact, besides recycling CO<sub>2</sub>, the

---

✉ Paolo Tosi  
paolo.tosi@unitn.it

<sup>1</sup> Dipartimento di Fisica, Università di Trento, Via Sommarive 14, 38123 Povo, Trento, Italy

<sup>2</sup> PLasMI Lab., CNR NANOTEC, Via Amendola 122/D, 70126 Bari, Italy

simultaneous efficient storage of renewable electricity in the chemical form would open the way for both an increasing share of intermittent energy sources and the electrification of the chemical industry.

Among the novel technologies proposed for the CO<sub>2</sub> conversion, the only one that currently parallels in performance a more mature technology as the water electrolysis is the plasma-chemical conversion, whose record solar-to-fuel efficiency, 23%, compares favourably with the 19% value of the water electrolysis [2].

Recently, and with increasing evidence, it has become clear that the key to the success of the plasma-chemical conversion of CO<sub>2</sub> lies in the non-equilibrium feature of cold plasmas [2, 3]. Although the dielectric barrier discharge is at the moment the most popular discharge for the plasma conversion of CO<sub>2</sub> [4–9], we decided to exploit a plasma characterised by a higher degree of non-equilibrium, namely a Nanosecond Repetitively Pulsed discharge (NRP). Understanding the promising results achieved by using the NRP [10] requires a thorough study of the microscopic processes occurring in the plasma. For this purpose, we have investigated the time evolution of CO<sub>2</sub> dissociation in the post-discharge by time-resolved Laser Induced Fluorescence (LIF) diagnostics. In such an approach, the discharge is no longer a “black box”, since we can investigate what happens in the time interval between each pair of pulses.

In this paper, we show results on the fragmentation kinetics of CO<sub>2</sub> on the  $\mu$ s scale in the post-discharge by performing Collisional Energy Transfer LIF, CET-LIF, [11] on the OH radical, which is used as a *probe* molecule. The OH radical is produced in the discharge by adding trace H<sub>2</sub>O to CO<sub>2</sub>. Our data indicate that the final CO<sub>2</sub> dissociation, i.e. the one observed in the exhaust of the reactor, is much lower than that found immediately after a single discharge event. As a consequence, much room exists for improvements in the process performance.

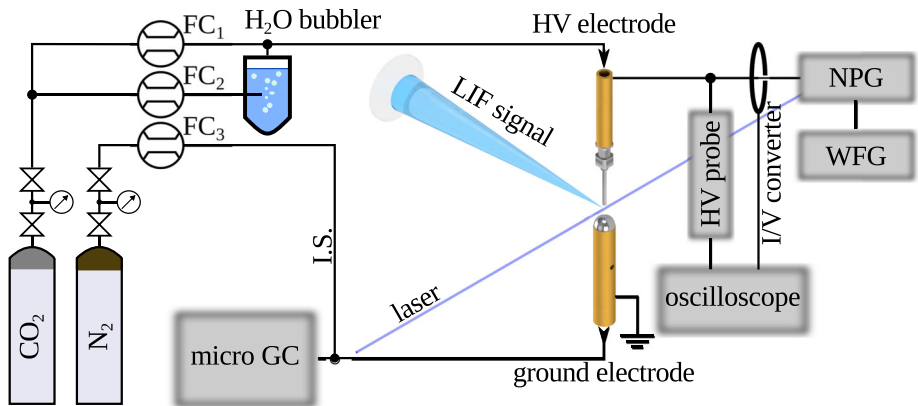


**Fig. 1** Schematic representation of the experimental setup. FC1, FC2 and FC3: mass flow controllers (1179, MKS) with 500, 200 and 1000 sccm full scale, respectively; WFG waveform generator, NPG nanosecond power supply, HV probe high voltage probe, I.S. internal standard IS

## Experimental

### Discharge Apparatus

The plasma driven CO<sub>2</sub> conversion was carried out in a pin-to-sphere configuration, see Fig. 1. It is worth to note that we have chosen this electrode arrangement because it is suitable to be coupled with the LIF diagnostic, and not to get the maximum conversion value.

The high voltage (HV) electrode was a stainless steel tube (internal diameter 1.2 mm, external diameter 1.65 mm), which also acted as inlet gas line. The grounded electrode was a stainless steel sphere (8 mm in diameter) placed in front of the needle. The inter-electrode gap was set at 5 mm.

NRP discharges were produced by an NPG 18/3500 power supply, (Megaipulse Ltd.), triggered by a wave-form generator (33220A, Agilent). In this work, the pulse repetition rate  $f_p$  ranged from 900 to 3000 Hz. The applied voltage  $V(t)$  and the current  $I(t)$  flowing in the discharge were measured by a high voltage probe (P6015A, Tektroniks) and an I/V converter (CT-D1.0, Magnelab), respectively. A digital oscilloscope (WaveSurfer 104MXs-A, LeCroy) was used to record  $I(t)$  and  $V(t)$ . The energy delivered by each pulse  $E_p$  was calculated as the time integral of the product of the measured voltage  $V(t)$  and current  $I(t)$ . The spurious time delay between  $I(t)$  and  $V(t)$  was measured when no breakdown occurred and appropriately taken into account [10].

Two mass flow controllers set the CO<sub>2</sub> input flow. A CO<sub>2</sub> stream flowed through a water vessel kept at 15 °C, then was furtherly diluted by a dry CO<sub>2</sub> stream. The total CO<sub>2</sub> flow through the HV needle was 100 sccm. The water vapour content in the inlet gas was 1.35%, partial pressure 10 Torr, for a total pressure of 735 Torr.

### Effluent Gas Analysis

A two channels gas chromatograph (GC) equipped with a thermal conductivity detector (3000 Micro GC, Agilent) is placed in the exhaust gas line for in-line analysis. N<sub>2</sub> (9%) was added to the exhaust gas as an internal standard (IS) to take into account the mole variation due to the CO<sub>2</sub> dissociation. After external standard calibration, nitrogen, carbon monoxide and hydrogen were quantified by a Molsieve 5A column with back-flush, whereas carbon dioxide was quantified by a PLOT U column. Argon was used as a gas carrier. GC analysis was run before and during each plasma process. The CO<sub>2</sub> conversion ( $C_{CO_2}$ ) is calculated as:

$$C_{CO_2}(\%) = \frac{n_{CO_2}^{in}(mol) - n_{CO_2}^{out}(mol)}{n_{CO_2}^{in}(mol)} \cdot 100 \quad (1)$$

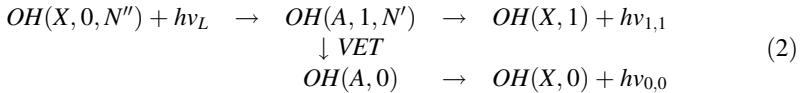
where  $n_{CO_2}^{in}$  and  $n_{CO_2}^{out}$  are the measured input and output CO<sub>2</sub> mol.

### Laser Induced Fluorescence Apparatus and Method

We already presented the LIF setup in [12], and the reader can refer to that paper. For the time-resolved LIF measurements, we used a discharge pattern made of pulse bursts repeated at a frequency of 300 Hz, corresponding to a burst period of  $T_b = 3.33$  ms. Each burst was composed of 4 pulses, each other separated by  $T_p = 333$  μs, corresponding to a pulse frequency inside the burst of 3 kHz. A digital delay generator synchronised the laser

firing with the discharge pattern. LIF measurements on the OH radical were carried out at 10 Hz as a function of the time delay  $t_d$  from the last pulse of the corresponding burst, see Fig. 2.

By LIF spectroscopy we can obtain information on both temperature and composition of the gas. For OH, we used the classical LIF scheme [12]



The gas temperature  $T$  can be measured by recording the excitation spectrum of OH, i.e. the spectrum obtained by scanning the laser frequency and recording the fluorescence with a fixed spectral window including, in our case, the entire (0, 0) and (1, 1) bands. In such a way the different rotational levels  $N''$  of OH( $X$ ) are probed, whose population is determined by the gas temperature (given the equality  $T_{\text{rot}} = T$  for OH( $X$ )). We used the transitions  $R_2(9)$  at 2817.32 Å,  $R_1(11)$  at 2817.38 Å,  $R_2(4)$  at 2817.57 Å, and  $R_{2,1}(11)$  at 2817.59 Å and we fitted the experimental spectrum with a synthetic spectrum with  $T$  as a free parameter. The present choice of transitions includes quite high rotational numbers, and is more suitable for temperatures higher than 1000 K than the set of transitions used in [12] that were chosen for temperature measurement in a cold plasma jet.

Due to the collisions with the surrounding molecules  $M$ , the fluorescence photons are emitted from levels other than the single state OH( $A, 1, N'$ ) populated by the laser. In particular, the rotational energy transfer process, RET, populates rotational levels other than  $N'$  in OH( $A, 1$ ) and eventually generates the fluorescence  $h\nu_{1,1}$ , while the vibrational energy transfer process, VET, OH( $A, 1$ ) +  $M$  → OH( $A, 0$ ) +  $M$  populates the OH( $A, 0$ ) that produces the fluorescence  $h\nu_{0,0}$ . The gas composition affects the LIF spectrum because the single state initially excited by the laser is depopulated non-radiatively by collisions with the background gas. Since the frequency of the energy transfer processes strongly depends on the collision partner [13], different gas mixtures give rise to distinct

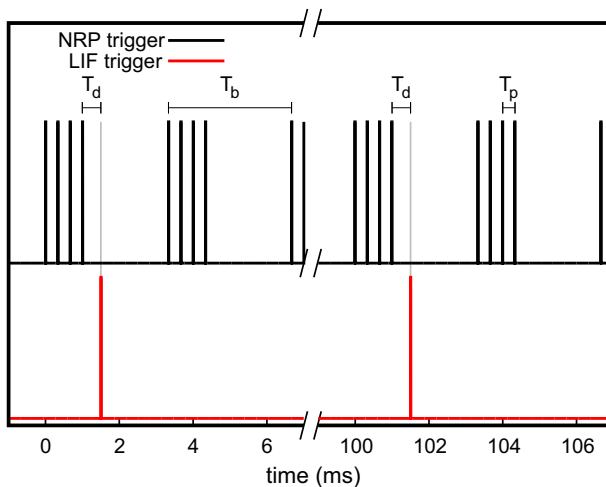


**Fig. 2** Temporal pattern of the discharge (upper graph) and laser firing trigger (lower graph). The discharge operated in burst mode (burst period  $T_b = 3.33$  ms; pulse to pulse period  $T_p = 333$  μs), the LIF measurement was carried out at a variable delay  $t_d$  respect to the last pulse of the burst every 100 ms

fluorescence spectra. Thus in principle, one can infer the gas composition if the relevant rate coefficients are known. Such a procedure has been described in [11]. The ratio between the (1, 1) and (0, 0) bands depends on the CO<sub>2</sub> dissociation. The conversion of CO<sub>2</sub> to CO and O<sub>2</sub> lowers the VET effectiveness since both CO and O<sub>2</sub> are collisional partners *M* less efficient than CO<sub>2</sub> for the vibrational energy transfer process OH(A, 1) + *M* → OH(A, 0) + *M*. In particular, the band ratio depends only on the rate coefficient ratio  $k_{\text{VET}}/k_{\text{Q0}}$  [11], where  $k_{\text{VET}}$  is the effective (dependent on the gas composition) VET rate coefficient, and  $k_{\text{Q0}}$  is the effective rate coefficient for the quenching of the OH(A, 0) state. By fitting the LIF spectrum using the 5-level model described in [12], the ratio  $k_{\text{VET}}/k_{\text{Q0}}$  can be inferred and eventually the gas composition can be calculated once the collisional rate coefficients are known. This is the CET-LIF procedure we have presented in [11].

It is worth to underline that the sole dependence on the  $k_{\text{VET}}/k_{\text{Q0}}$  ratio makes the procedure independent of the absolute concentration of the gas components. This fact is crucial in our specific case, in which the discharge channel has an explosive behaviour, i.e. a fast gas heating, in the first few ns, up to 2000–2500 K temperatures, followed by gas expansion and cooling in the tens of  $\mu\text{s}$  timescale.

There are two points to address before CET-LIF can give fully quantitative outcomes. Both points arise from the fact that reliable collisional data are available mainly at room temperature and for thermalised rotational distributions of OH(A, 0 – 1) [13].

The first point is due to the rate coefficient dependence on the rotational levels. Rotational thermalisation requires a sufficient number of RET collisions within the lifetime of the vibro-electronic state. In a mixture of CO<sub>2</sub>, CO and O<sub>2</sub> as main components, this is not achieved, since the rapid collision quenching shortens too much the lifetime. Both OH(A, 1) and OH(A, 0) present a non-Boltzmann rotational distribution, since: OH(A, 1) starts from a nascent distribution in which only one rotational level is populated by laser light absorption; OH(A, 0) starts from a highly supra-thermal distribution generated by the VET population process [11, 14]. A detailed knowledge of the the actual rotational distribution of the OH(A) state and of specific rate coefficients related to those rotational distributions is then required. From now on we call these specific rate coefficients with the adjective “non-thermal”. Such a measurement campaign is in due course.

The second point is the temperature dependence of the rate coefficients, that might induce a temperature dependence of the  $k_{\text{VET}}/k_{\text{Q0}}$  ratio, or of the cross sections, given that  $k_{\text{VET}}/k_{\text{Q0}} = \sigma_{\text{VET}}/\sigma_{\text{Q0}}$ . Here we deal only with “temperature averaged” cross sections. This issue is critical in our case since in the discharge pulse, as we shall see, the temperature rises to about 2500 K and then decreases to about 1000 K in the after-pulse. The temperature dependence is determined by the interaction between OH(A) and the collider. The latter, being governed by attractive forces, gives rise to the following law for the temperature averaged cross section as a function of *T* [15–17]:

$$\sigma = \sigma_{\infty} \exp(\epsilon/kT). \quad (3)$$

where  $\epsilon$  is related to the well depth of the attractive potential and  $\sigma_{\infty}$  is the value at very high *T*. The  $\epsilon/k$  value, determined in [16] for the quenching of (A, *v* = 0), is equal to 488, 397 and 243 K for CO<sub>2</sub>, CO and O<sub>2</sub> respectively. As a consequence, in the range 1400–2500 K (that is the temperature variation of our measurements), the temperature dependence of the cross section is rather smooth and small (see also the collection of measurements reported in [15]). Should this law be strictly true, both VET and quenching would have the same dependence on *T*, since the well depth for low *v* is negligibly affected

by the vibrational state, such that the ratio  $\sigma_{\text{VET}}/\sigma_{\text{Q0}}$  is independent on T. Actually, although this conclusion appears reasonable and the law (3) has been found to provide a good fit to the available data at different temperatures for the ( $A, v = 0$ ) quenching [16], it has no true experimental demonstration. VET cross sections measurements exist at ambient temperature (see [11] and references therein), including a data set at 195–294 K [17], and for high temperatures in a shock tube at 1900 and 2300 K [18]. A larger data set exists for quenching cross sections, for which law (3) has been tested [16]. In [18] it was noted that the cross sections do not change appreciably from 1900 to 2300 K and that, for  $\text{CO}_2$  collider, the ratio  $\sigma_{\text{VET}}/\sigma_{\text{Q0}}$  at high temperature is substantially the same as that at 300 K.

It is clear that this issue requires further investigation. At the present status of the knowledge, and for the present purposes, we conclude that the ratio  $\sigma_{\text{VET}}/\sigma_{\text{Q0}}$  is independent of T and equal to the value at  $T = 300$  K in the best case, while in the worst case it is reasonably independent of T, in the temperature range 1400–2500 K of our concern, and with a value that can be slightly different from that at  $T = 300$  K.

Waiting for fully clarifying these issues, it is nevertheless possible to establish a procedure based on the current knowledge to estimate the gas composition. The method is based on the following assumptions: a) the  $k_{\text{VET}}/k_{\text{Q0}}$  ratio is independent on T; b) the non-thermal  $k_{\text{VET}}/k_{\text{Q0}}$  ratio can be determined by measuring spectra of pure gases in a cell at  $T = 300$  K; c) the differences between thermal and non-thermal  $k_{\text{VET}}/k_{\text{Q0}}$  ratios are due mainly to variations of  $k_{\text{Q0}}$ .

Assumption (a) has been already justified, while points (b) and (c) are discussed in the following.

The starting point is that fluorescence spectra recorded from a gas cell at room temperature with pure gases [11] can be used to estimate the non-thermal  $k_{\text{VET}}/k_{\text{Q0}}$  ratios, once the rotational distributions of both  $\text{OH}(A, 1)$  and  $\text{OH}(A, 0)$  are guessed, as in [11]. Two spectra are shown in Fig. 4b, for comparison with spectra measured in the discharge. They refer to the cases of pure  $\text{CO}_2$  and pure CO. As a rough guess of the rotational distribution of  $\text{OH}(A, 0)$ , we have used a Boltzmann one at  $T_{\text{rot}} = 1500$  K. Such a guess, at the present spectral resolution, appears to be equally good for both  $\text{CO}_2$  and CO. The case of pure  $\text{O}_2$  is almost identical to that of CO, so that it is not reported in the figure to avoid confusion (note that, from the data of [13], the thermal  $k_{\text{VET}}/k_{\text{Q0}}$  ratio is practically the same for CO and  $\text{O}_2$ ). Then, the CO case spectrum of Fig. 4b is, with very good approximation, what is expected in the case of full  $\text{CO}_2$  dissociation into CO and  $\text{O}_2$ . We underline that the estimate of the non-thermal  $k_{\text{VET}}/k_{\text{Q0}}$  ratio depends on the rotational distribution guess for  $\text{OH}(A, 0)$  state. Having chosen the same guess for the three pure gases can be a source of error in the estimation of the gas composition, i.e. the absolute  $\text{CO}_2$  dissociation. Nevertheless, the relative time evolution of the band ratio after the discharge pulse should not be affected, since no significant change in the rotational distributions is observed along the time.

Finally, we point out that differences between thermal and non-thermal  $k_{\text{VET}}/k_{\text{Q0}}$  ratios must very likely be attributed mainly to variations of  $k_{\text{Q0}}$  only. As reported in [11], both  $k_{\text{VET}}$  and the rotational distribution of  $\text{OH}(A, 0)$  do not depend appreciably on the rotational level excited by the laser, i.e. they appear to be independent on the rotational distribution of  $\text{OH}(A, 1)$ . On the other hand, as pointed out in [13], the thermal quenching, due to fast RET transfers, is dominated by the faster quenching rates of low J-levels. In the present non-thermal case, in which RET rates are slower than the quenching, the quenching rate corresponds to an average of individual J-levels quenching rates, such that slowly quenched J-levels contribute much to the value averaged over the rotational distribution.

Although this hypothesis is reasonable, it can be another source of error, We return on this point later, showing how much it can affect the gas composition estimation.

In summary, the use of the empirical non-thermal  $k_{VET}/k_{Q0}$  ratios at  $T = 300\text{ K}$  to analyse the band ratio values and obtain the gas composition does not affect the temporal behaviour of the gas mixture in the after-pulse, while it may affect its absolute value by an amount that we shall try to estimate. The mixture composition found in the effluent gas by GC measurements is a reference to compare with CET-LIF estimations.

## Results and Discussion

### Effluent Products and Final CO<sub>2</sub> Conversion

The main products of discharge treatment were CO and O<sub>2</sub>. A negligible amount of H<sub>2</sub> was detected ( $< 0.05\%$ ). Although powders were found in the reactor, the carbon balance is always higher than 98%. We report in Fig. 3 the CO<sub>2</sub> conversion as a function of the specific energy input (SEI) calculated as:

$$SEI(\text{kJ dm}^{-3}) = \frac{P_d(\text{W})}{\phi_r(\text{cm}^3 \text{ s}^{-1})} = \frac{\widetilde{E}_p(\text{J})f_p(\text{Hz})}{\phi_r(\text{cm}^3 \text{ s}^{-1})}, \tag{4}$$

$$SEI(\text{kJ mol}^{-1}) = \frac{P_d(\text{W})}{\phi_r(\text{cm}^3 \text{ s}^{-1})22.4(\text{dm}^3 \text{ mol}^{-1})} = \frac{\widetilde{E}_p(\text{J})f_p(\text{Hz})}{\phi_r(\text{cm}^3 \text{ s}^{-1})22.4(\text{dm}^3 \text{ mol}^{-1})} \tag{5}$$

where  $P_d$  is the discharge power,  $\widetilde{E}_p$  is the mean discharge pulse energy calculated averaging 500  $E_p$ ,  $\phi_r$  is the standard flux of reactant gases. The SEI value is varied by

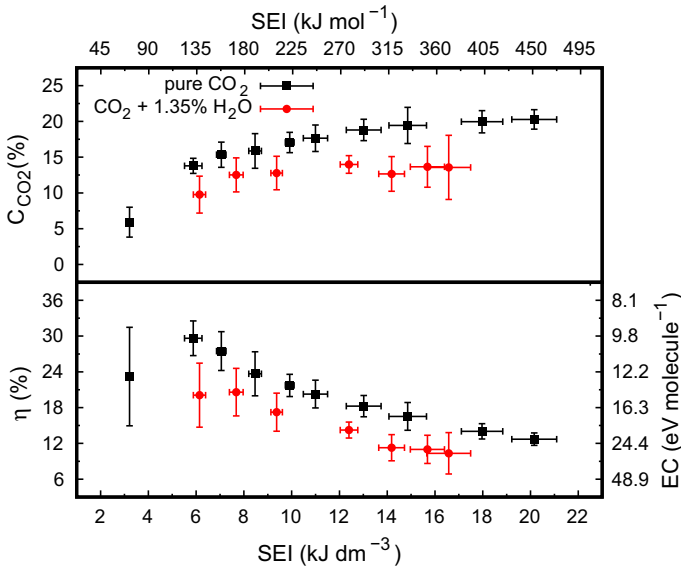


**Fig. 3** Conversion of CO<sub>2</sub> in dry and humid condition (upper graph), energy conversion efficiency  $\eta$  and energy cost  $EC$  (lower graph) as a function of SEI. Measurement in the effluent gas by gas chromatography (GC)

acting both on the discharge voltage, i.e. on the pulse energy, and on the frequency. The conversion comes out to be dependent on the SEI value only. In the same figure the energy conversion efficiency  $\eta$  and the energy cost  $EC$  are shown:

$$\eta = \frac{C_{CO_2} \Delta H_{300\text{K}}^0 (\text{kJ mol}^{-1})}{SEI (\text{kJ mol}^{-1})} \quad (6)$$

$$EC (\text{eV molecule}^{-1}) = \frac{SEI (\text{kJ mol}^{-1}) 6.24 \cdot 10^{21} (\text{eV kJ}^{-1})}{C_{CO_2} 6.022 \cdot 10^{23} (\text{molecule mol}^{-1})} \quad (7)$$

where  $\Delta H_{300\text{K}}^0 = 283 \text{ kJ mol}^{-1}$  is the reaction enthalpy for pure  $\text{CO}_2$  splitting [2].

In Fig. 3, data are reported for dry  $\text{CO}_2$  and for humid  $\text{CO}_2$  with the addition of 1.35% of  $\text{H}_2\text{O}$ . The primary purpose of water addition is to compare effluent gas conversion to CET-LIF outcomes. Interestingly we note that water addition lowers  $\text{CO}_2$  conversion and anticipates its saturation behaviour on increasing SEI. In [10] we argued a role of water formation as a limiting factor for the conversion. Specific studies are needed to clarify this issue.

## LIF Results: $\text{CO}_2$ Conversion

First, we point out that all LIF measurements start at a delay of  $4 \mu\text{s}$  after the discharge pulse. Earlier delays cannot at present be reached due to the overwhelming light emission generated by the discharge itself that blinds the detectors. Measurements are reported until a useful LIF signal could be recovered. Due to OH concentration decrease, after  $150 \mu\text{s}$  the signal drops too much for reliable signal analysis.

The CET-LIF procedure shows a significant variation of the gas composition as a function of the time after a discharge pulse. An example of the fluorescence spectra at two different time-delays is shown in Fig. 4. It is evident that the ratio between the (0, 0) and (1, 1) bands increases as a function of time, indicating an increasing efficiency of the VET processes. The post-discharge spectra in comparison with the pure gases spectra measured in a cell, appear to be intermediate between the two pure gases one, or, in other words, between the full and null  $\text{CO}_2$  dissociation. The  $k_{\text{VET}}/k_{\text{QO}}$  ratio time evolution, deduced from the LIF spectra, after the last discharge pulse in the burst is reported in Fig. 5.

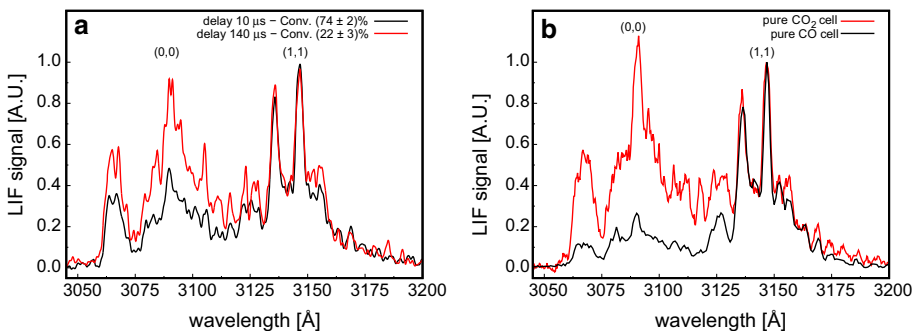


**Fig. 4** **a** Fluorescence spectra in the  $\text{CO}_2 + 1.35\% \text{H}_2\text{O}$  NRP discharge at two delays from the last pulse of the burst.  $SEI = 7.2 \text{ kJ dm}^{-3}$ . **b** Spectra measured in a cell at room temperature filled with  $\text{CO}_2$  (red) and  $\text{CO}$  (black), and with a very small addition of  $\text{H}_2\text{O}_2 + \text{H}_2\text{O}$ . The laser is tuned to the  $P_1(3)$  line



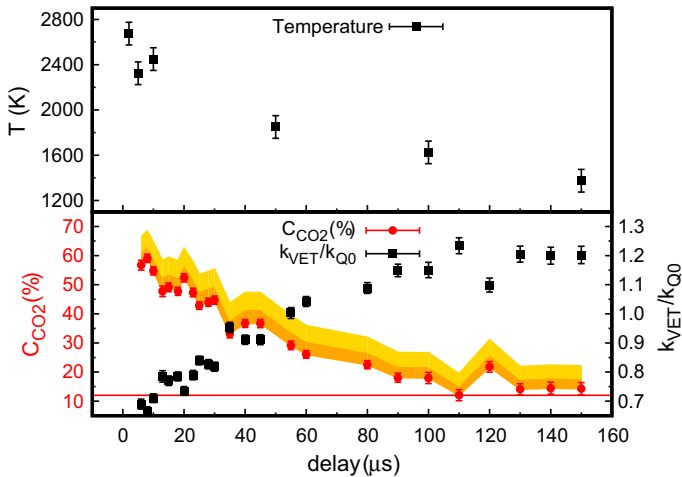


**Fig. 5** Temperature,  $k_{Q0}/k_{VET}$  and  $C_{CO_2}$  as a function of the delay after the last pulse of the burst. Gas composition  $CO_2 + 1.35\% H_2O$ ,  $SEI = 7.2 \text{ kJ dm}^{-3}$ .  $CO_2$  splitting causes a decrease of the  $k_{VET}/k_{Q0}$  ratio. The 12%  $CO_2$  dissociation in the effluent gas measured by GC is reported as a red horizontal line

According to the discussion of par. 2.3 we are allowed to explain it as mostly due to a change in the gas composition, i.e. to the conversion of  $CO_2$  into  $CO$  and  $O_2$ .

### LIF Results: Gas Temperature

Examples of experimental excitation spectra fitted by synthetic ones at the appropriate temperature are plotted in Fig. 6 at increasing time-delays from the discharge. The change of lines ratio corresponding to the temperature range is evident. The evolution of  $T$  in the post-pulse is reported in Fig. 5. Error bars are calculated by the fitting algorithm.  $T$  varies in the range from around 2500 K at 5  $\mu\text{s}$  after the discharge down to around 1400 K after around 150  $\mu\text{s}$ . Again, at higher delays, the LIF signal decreases too much for a reliable measurement. The timescale of gas cooling is comparable to that of gas expansion after its fast heating in the discharge [19]. The expansion is followed by recirculation of cold surrounding gas, that might be one of the possible causes for the decrease of the “local” dissociation degree in the region sampled by the laser.

### LIF Results: Discussion

The most important finding is the substantial variation of the gas composition in the post-discharge. In addition, we have tried to quantify the  $CO_2$  dissociation according to the procedure detailed in Sect. 2.3, to get a reasonable idea of the quantities involved. The  $k_{VET}/k_{Q0}$  ratio, in the hypothesis of its temperature independence in the high-temperature range of the measurements, correctly represents the relative time evolution of the gas composition, while the absolute  $CO_2$  dissociation value is somewhat influenced by the choices made in the analysis of the spectra in the cell filled with pure gases. In Fig. 5 we report the dissociation values calculated with the procedure of “[Laser Induced Fluorescence Apparatus and Method](#)” section, The red points are those calculated assuming that the whole difference between the thermal and the non-thermal  $k_{VET}/k_{Q0}$  ratios is due to a

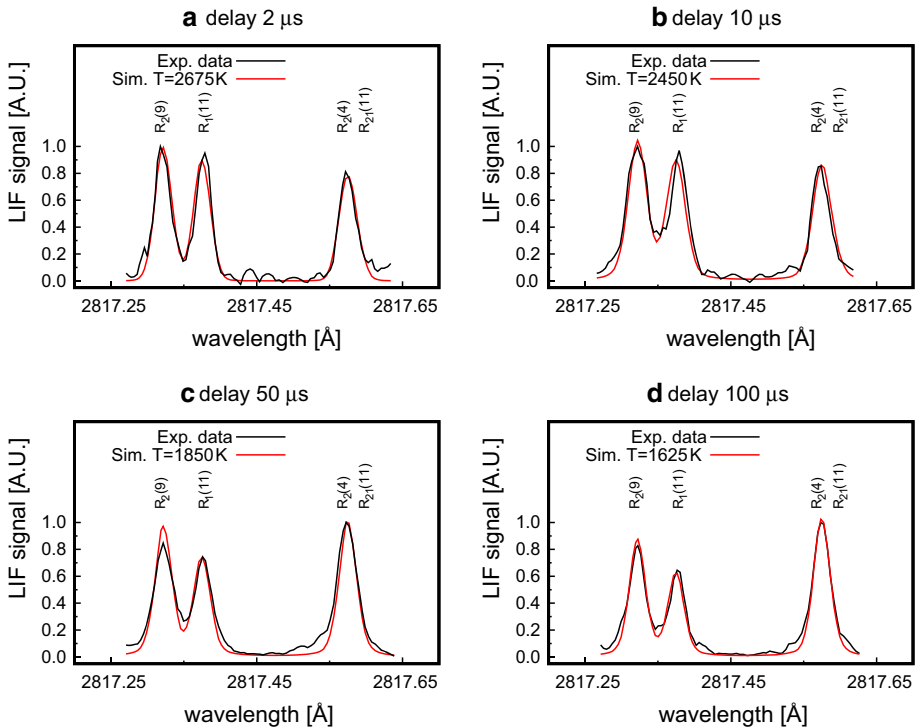


**Fig. 6** Excitation spectra of OH at different delays with respect to the last discharge of a burst. Gas composition  $\text{CO}_2 + 1.35\% \text{H}_2\text{O}$ ,  $\text{SEI} = 7.2 \text{ kJ dm}^{-3}$

variation of  $k_{\text{Q0}}$  only. Although very reasonable, can be somewhat incorrect. To look for the effect of a different choice, we have calculated the dissociation values in the cases: (a) the difference is equally shared between  $k_{\text{VET}}$  and  $k_{\text{Q0}}$  (dark shadow); (b) the difference is attributed to  $k_{\text{VET}}$  only (light shadow). In Fig. 5, it is also reported the dissociation value of about 12% found in the effluent gas at the same  $\text{SEI} = 7.2 \text{ kJ dm}^{-3}$  by GC measurements. There are many reasons for which this value can be lower than it is at  $150 \mu\text{s}$  in the after-pulse: a further decrease in the post-pulse due to still evolving chemical kinetics; the further cooling of the gas; the fact that the discharge pulses sequence in the burst may not fill the entire gas volume, such that a lower dissociation value in GC measurements gas can be due to the presence of an “untreated” part of gas. Certainly, the  $\text{C}_{\text{CO}_2}$  value of the effluent gas cannot be larger than the value at  $150 \mu\text{s}$  in the post-discharge. It then represents a lower limit for the  $\text{CO}_2$  dissociation estimated by CET-LIF.

Finally, and thanks to this lower limit, if we put into question the main hypothesis of temperature independence of the  $k_{\text{VET}}/k_{\text{Q0}}$  ratio, and attribute the  $k_{\text{VET}}/k_{\text{Q0}}$  variation in the post discharge to the temperature change, we are led to rather odd conclusions: most (about a factor of 2) of the  $k_{\text{VET}}/k_{\text{Q0}}$  change with temperature must occur in the temperature range 1400–2500 K, while a minimal change should occur in the range 300–1400 K. This is exactly the opposite of the temperature dependence of law (3). Reminding that law (3) is experimentally verified for the cross sections of the quenching of  $(A, v = 0)$ , we should conclude that the VET cross section must have quite an exotic dependence on  $T$ , with a monotonic decrease at least up to 2500 K.

It is important to correlate the results obtained for the temperature and the dissociation. Allowing for data scattering, temperature measurement errors and the fact that our measurements start 4  $\mu\text{s}$  after the discharge, we can set a maximum value of the temperature at about 2800 K. In a thermal process, the dissociation value at 2800 K is about 31%, and even at 3000 K it raises to 46% (see Fig. 2 in [2]). A few  $\mu\text{s}$  after the pulse, the  $\text{CO}_2$  dissociation estimated by CET-LIF analysis is about 60% at 2500 K, see Fig. 5, or even larger if we move into the shadowed area. With all the caution related to the uncertainty of the CET-LIF analysis, and given that equilibrium concentrations in a thermal process may not be valid in this fast transient system, we feel encouraged to think that important non-equilibrium mechanisms are at work in the ns discharge.

## Conclusions

The main result of the present paper is the disclosure of time evolution of the  $\text{CO}_2$  dissociation after a discharge pulse. In comparison to the dissociation degree measured in the effluent gas at the exit of the reactor, we observe in the near post-pulse a much higher value that successively decreases by about a factor of three. Of course, this finding indicates room for improvements that relies on understanding the causes of such a decrease: (a) fluid-dynamic—remixing with “untreated” gas after fast expansion of the discharged volume; (b) chemical back-reactions; (c) still too slow cooling of the gas.

Insights into these issues can be achieved thanks to time-resolved, local diagnostics again. The precious help of LIF has been shown here, as a tool that opens a window in the “black box” of a plasma gas treatment, but also how much this technique is complicated and even now in need of fundamental data. So much so that the full quantitative application of CET-LIF still requires investigations on the non-thermal collision rate coefficients and their temperature dependence. We indeed believe that efforts are worth in this direction, and in general, in the development of diagnostic techniques in such a harsh environment.

A final consideration concerns the non-equilibrium contribution to the conversion. Though at present we cannot quantify the latter, as we still are not able to extract accurate absolute values of the dissociation from CET-LIF outcomes, there are some hints that non-equilibrium dissociation can be significant.

**Acknowledgements** L M Martini acknowledges financial support from Fondazione Cassa di Risparmio di Trento e Rovereto, Grant Bando 2016 per progetti di ricerca scientifica svolti da giovani ricercatori post-doc.

## References

1. Navarrete A, Centi G, Bogaerts A, Martín À, York A, Stefanidis GD (2017) *Energy Technol* 5:796–811
2. Snoeckx R, Bogaerts A (2017) *Chem Soc Rev* 46:5805–5863
3. Taccogna F, Dilecce G (2016) *Eur Phys J D* 70:251–287
4. Scarduelli G, Guella G, Ascenzi D, Tosi P (2011) *Plasma Process Polym* 8:25–31
5. Martini LM, Dilecce G, Guella G, Maranzana A, Tonachini G, Tosi P (2014) *Chem Phys Lett* 593:55–60
6. Scapinello M, Martini LM, Tosi P (2014) *Plasma Process Polym* 11:624–628
7. De Bie C, van Dijk J, Bogaerts A (2016) *J Phys Chem C* 120:25210–25224
8. Ozkan A, Bogaerts A, Reniers F (2017) *J Phys D Appl Phys* 50:084004
9. Wang L, Yi Y, Wu C, Guo H, Tu X (2017) *Angew Chemie*. <https://doi.org/10.1002/anie.201707131>
10. Scapinello M, Martini LM, Dilecce G, Tosi P (2016) *J Phys D Appl Phys* 49:075602–075609
11. Martini LM, Gatti N, Scotoni M, Dilecce G, Tosi Paolo (2018) *Plasma Phys. Control Fusion* 60:014016

12. Dilecce G, Martini LM, Tosi P, Scotoni M, De Benedictis S (2015) *Plasma Source Sci Technol* 24:034007
13. Martini LM, Gatti N, Dilecce G, Scotoni M, Tosi P (2017) *J Phys D Appl Phys* 50:114003
14. Copeland RA, Wise ML, Crosley DR (1988) *J Phys Chem* 92:5710–5715
15. Paul PH (1994) *J Quant Spectrosc Radiat Transf* 51:511–524
16. Tamura M, Berg PA, Harrington JE, Luque J, Jeffries JB, Smith GP, Crosley DR (1998) *Combust Flames* 114:502–514
17. Steffens KL, Crosley DR (2000) *J Chem Phys* 112:9427–9432
18. Paul PH (1995) *J Phys Chem* 99:8472–8476
19. Castela M, Stepanyan S, Fiorina B, Coussement A, Gicquel O, Darabiha N, Laux CO (2017) *Proc Combust Inst* 36:4095–4103